Gazi Üniversitesi
Fen Bilimleri Dergisi
PART C: TASARIM VE TEKNOLOJİ

Gazi University
Journal of Science
PART C: DESIGN AND TECHNOLOGY

GU J Sci, Part C, 13(2): 538-552 (2025)

Effects of Adhesive Type and Surface Preparation on the Mechanical Strength of Thermoplastic and CFRP Structures

Emin ÖZTÜRK[1], Mert KILINÇEL[1*], Gülden KABAKÇI[2], Ahmet KÖMÜRCÜ[1]

[1]*Duzce University, Faculty of Engineering, Department of Mechanical Engineering, Duzce, Turkey*

[2]*Düzce University, Department of Mechanical Engineering, Düzce Vocational School, Düzce, Türkiye*

Article Info

Research article
Received: 23/01/2025
Revision: 28/03/2025
Accepted: 06/04/2025

Keywords

Composite
Thermoplastic
Thermoset
Mechanical Strength
Adhesive Type
Surface Preparation

Makale Bilgisi

Araştırma makalesi
Başvuru: 23/01/2025
Düzeltme: 28/03/2025
Kabul: 06/04/2025

Anahtar Kelimeler

Kompozit
Termoplastik
Termoset
Mekanik Dayanım
Yapıştırıcı Türü
Yüzey Hazırlığı

Graphical/Tabular Abstract (Grafik Özet)

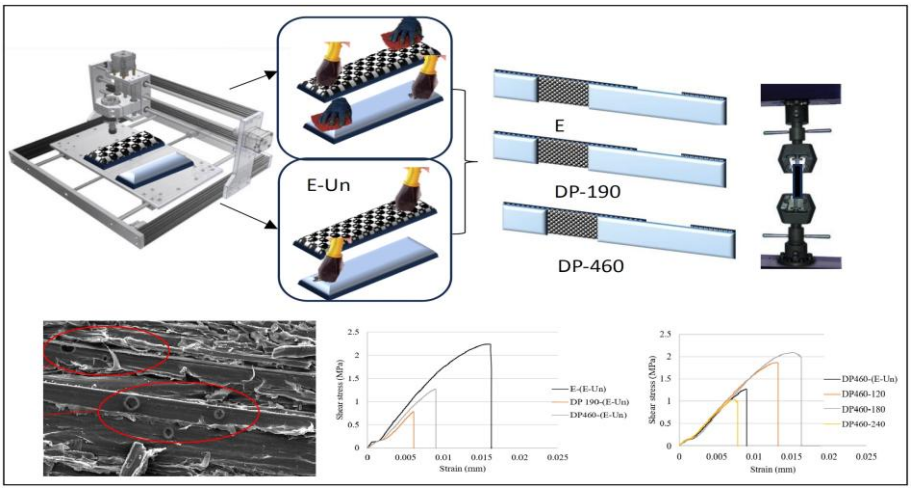

***Figure A**: Shear strength comparison of adhesives on HDPE-CFRP joints. /**Şekil A:**.HDPE-CFRP birleşimlerinde yapıştırıcıların kesme dayanımı karşılaştırması*

Highlights (Önemli noktalar)

- *HDPE-CFRP birleşimlerinde yapıştırıcı türü ve yüzey hazırlığının mekanik dayanım üzerindeki etkisi incelenmiştir. /The effect of adhesive type and surface preparation on the mechanical strength of HDPE-CFRP joints was examined.*
- *Tüm yapıştırıcılar arasında 120 numara zımparayla uygulanan DP190 en yüksek kesme dayanımını (~25 MPa) göstermiştir. / Among all adhesives, DP190 with 120-grit sanding showed the highest shear strength (~25 MPa).*
- *Epoksi dengeli bir performans sergilerken, DP460 HDPE'ye karşı zayıf yapışma göstermiştir. / Epoxy achieved balanced performance, while DP460 exhibited insufficient bonding to HDPE.*

Aim (Amaç): *To investigate the effects of adhesive type and surface preparation on the mechanical performance of CFRP-HDPE joints. / CFRP ve HDPE birleşimlerinde yapıştırıcı türü ve yüzey hazırlığının mekanik performansa etkisinin araştırılması amaçlanmıştır.*

Originality (Özgünlük): *This study provides a comparative mechanical analysis of different adhesive systems (epoxy, DP190, DP460) with controlled surface preparations for CFRP-HDPE bonding, including SEM-supported failure mechanisms. / Bu çalışma, CFRP-HDPE yapıştırma uygulamalarında farklı yapıştırıcı sistemlerinin (epoksi, DP190, DP460) kontrollü yüzey hazırlıklarıyla karşılaştırmalı mekanik analizini ve SEM destekli hasar incelemesini sunmaktadır.*

Results (Bulgular): *DP190 demonstrated superior bonding strength (~25 MPa) with 120-grit sanding, while DP460 failed to bond effectively with HDPE. Epoxy showed moderate bonding with balanced elongation and strength. / DP190, 120 numara zımparalama ile üstün yapışma dayanımı (~25 MPa) gösterirken, DP460 HDPE'ye etkili şekilde yapışamamıştır. Epoksi ise dengeli uzama ve dayanım ile orta seviyede bir yapışma sergilemiştir.*

Conclusion (Sonuç): *Surface preparation is critical for improving adhesive bonding in CFRP-HDPE joints. DP190 is identified as the most suitable adhesive, while DP460 should be avoided for flexible thermoplastic bonding. / CFRP-HDPE birleşimlerinde yapıştırıcı performansını artırmada yüzey hazırlığı kritik öneme sahiptir. DP190 en uygun yapıştırıcı olarak öne çıkarken, DP460 esnek termoplastik yapıştırmalarda tercih edilmemelidir.*

*Corresponding author, e-mail: mertkilincel@duzce.edu.tr
DOI: 10.29109/gujsc.1625639

GU J Sci, Part C, 13(2): 538-552 (2025)

Gazi Üniversitesi
Fen Bilimleri Dergisi
PART C: TASARIM VE TEKNOLOJİ

Gazi University
Journal of Science
PART C: DESIGN AND TECHNOLOGY

http://dergipark.gov.tr/gujsc

Effects of Adhesive Type and Surface Preparation on the Mechanical Strength of Thermoplastic and CFRP Structures

Emin ÖZTÜRK[1], Mert KILINÇEL[1*], Gülden KABAKÇI[2], Ahmet KÖMÜRCÜ[1]

[1]*Duzce University, Faculty of Engineering, Department of Mechanical Engineering, Duzce, Turkey*

[2]*Düzce University, Department of Mechanical Engineering, Düzce Vocational School, Düzce, Türkiye*

Article Info

Research article
Received: 23/01/2025
Revision: 28/03/2025
Accepted: 06/04/2025

Keywords

Composite
Thermoplastic
Thermoset
Mechanical Strength
Adhesive Type
Surface Preparation

Abstract

Composite materials are widely used in industries for their lightweight, durability, and flexibility. Carbon fiber-reinforced composites are particularly demanded and used in aerospace, automotive, and space industries due to their high strength and low weight. They are also critical in manufacturing high-pressure hydrogen storage tanks, where the interfacial strength between thermoplastic and thermoset materials is crucial. This study investigates the effects of adhesive type and surface preparation on the mechanical strength of carbon fiber-reinforced composites bonded with high-density polyethylene (HDPE). Tensile tests were performed according to ASTM D5868, and scanning electron microscope (SEM) analyses were conducted to evaluate damage mechanisms. The results show that, DP 190-120 demonstrated the highest performance, providing a 108% higher shear stress (25 MPa) compared to other adhesives. In epoxy-bonded joints, the maximum shear stress (12 MPa) was observed in sample E-240. This value corresponds to only 48% of the performance of DP 190-240. Among the joints made with DP 460, DP 460-180 showed the best performance. However, with only 2.1 MPa shear stress, it reached just 8.4% of the performance of DP 190-180. These findings contribute to enhancing the safety of Type-IV hydrogen tanks and developing more reliable bonding methods for industrial applications.

Termoplastik ve CFRP Yapıların Birleştirilmesinde Yapıştırıcı Cinsi ve Yüzey Hazırlığının Malzemenin Mekanik Dayanımı Üzerindeki Etkileri

Makale Bilgisi

Araştırma makalesi
Başvuru: 23/01/2025
Düzeltme: 28/03/2025
Kabul: 06/04/2025

Anahtar Kelimeler

Kompozit
Termoplastik
Termoset
Mekanik Dayanım
Yapıştırıcı Türü
Yüzey Hazırlığı

Öz

Kompozit malzemeler, hafiflik, dayanıklılık ve esneklikleriyle birçok endüstride tercih edilmektedir. Havacılık, otomotiv ve uzay endüstrilerinde yaygın olan karbon fiber takviyeli kompozitler, yüksek dayanım ve düşük ağırlıklarıyla dikkat çekmektedir. Yüksek basınçlı hidrojen depolama tanklarının üretiminde de sıklıkla kullanılan bu malzemeler, termoplastik ve termoset yapıların birleşim bölgelerindeki dayanımlarıyla önem kazanmaktadır. Bu çalışmada, karbon fiber epoksi kompozitlerin yüksek yoğunluklu polietilen (HDPE) malzemelerle birleştirilmesinde yapıştırıcı türü ve yüzey hazırlığının mekanik dayanım üzerindeki etkileri araştırılmıştır. ASTM D5868 standardına uygun çekme testleri yapılmış, taramalı elektron mikroskobu (SEM) analizleriyle hasar mekanizmaları incelenmiştir. Sonuç olarak; DP 190-120 en yüksek performansı göstererek, diğer yapıştırıcılara göre %108 daha yüksek kesme gerilmesi (25 MPa) sağlamıştır. Epoksi ile yapılan birleşmelerde maksimum kesme gerilmesi (12 MPa) E-240 numunede gözlenmiştir. Bu değer, DP 190-240'ın performansının %48'ine karşılık gelmektedir. DP 460 ile yapılan birleştirmelerde DP 460-180 en iyi performansı göstermiştir. Ancak sadece 2.1 MPa kesme gerilmesi sağlayarak DP 190-DP 180'in performansının sadece %8.4'üne ulaşabilmiştir. Bu bulgular, Tip-IV hidrojen tanklarının güvenliğini artırmak ve endüstriyel uygulamalarda daha etkin birleştirme yöntemleri geliştirmek adına önemli bir katkı sunmaktadır.

1. INTRODUCTION (GİRİŞ)

In recent years, the diversification of industrial applications and increasing demand for advanced material properties have driven significant progress in material technologies [1]. Research in materials science and engineering has contributed substantially to the synthesis of new materials, enhancement of existing ones, and the joining of dissimilar materials [2–4]. Composite materials and

*Corresponding author, e-mail: mertkilincel@duzce.edu.tr
DOI: 10.29109/gujsc.1625639

thermoplastics are among the most widely studied and preferred materials in industrial applications [5, 6]. Composite materials—particularly carbon fiber-reinforced composites—are extensively used in aerospace, automotive, and defense industries due to their high strength-to-weight ratio [7–10]. Thermoplastics, such as high-density polyethylene (HDPE), are favored in structural mass production and advanced engineering applications (e.g., Type-IV hydrogen tank liners) because of their high strength and thermal conductivity [11–14].

Hydrogen tanks, critical to hydrogen storage technology, are classified into five types. Type-I, II, and III tanks are traditionally manufactured from metal alloys (e.g., stainless steel, aluminum), offering high strength and durability for safe hydrogen storage [15–17]. In contrast, Type-IV and Type-V tanks employ non-metallic materials. Type-IV tanks, designed for high mechanical and thermal resilience, consist of carbon fiber-reinforced composite shells over polymer liners [18–20]. Type-V tanks, fully composite and not yet commercialized, promise safer, more efficient, and cost-effective hydrogen storage, supporting the transition to sustainable energy [18].

Type-IV tanks provide pressure resistance at lower weights than metal tanks due to their low-density structure [19], enabling higher hydrogen storage capacity per volume. They also offer advantages such as lower production costs, superior corrosion/oxidation resistance, high fatigue strength, and extended service life compared to Type-I/II/III tanks [20]. However, hydrogen's high diffusivity leads to blister formation at material interfaces, weakening structural integrity and increasing explosion risks during depressurization [21, 23]. Such damage poses significant safety concerns [24–26], making blister mitigation critical for industrial safety standards [27]. Uncontrolled progression of these damage mechanisms may induce buckling, leading to catastrophic failure [28–30]. Studies are underway to reinforce interfaces and reduce blistering through adhesive bonding [31–33].

Another challenge in Type-IV tanks is thermal stress accumulation during filling/emptying cycles, necessitating improved thermal conductivity in liner materials [34–36]. Research has thus focused on enhancing thermal conductivity in liner design and manufacturing [37–39].

Literature highlights efforts to strengthen interfacial bonds in Type-IV tanks, particularly between thermoset composites and thermoplastics (e.g., HDPE) [40, 41]. A key challenge is achieving strong adhesion, as thermosets form a cross-linked 3D network upon curing, while thermoplastics exhibit linear/branched polymer chains, hindering chemical bonding. Solutions include chemical modifications (oxidation, plasma treatment), adhesives, and mechanical surface treatments [42, 43]. Epoxy-based adhesives, with their reactive functional groups, promote chemical bonding between thermoplastics and thermosets [44, 45]. Mechanical surface treatments (e.g., grinding) enhance adhesion by increasing roughness and mechanical interlocking, eliminating the need for chemical bonding [46].

Surface roughness directly influences adhesive performance [47]. Optimal roughness improves mechanical interlocking and bond strength, but excessive roughness causes stress concentrations and weakens the interface [48]. Studies investigating abrasive grit sizes provide critical data for determining optimal roughness values [49].

This study examines the mechanical strength of epoxy-bonded joints between carbon fiber-reinforced composites and thermoplastics (HDPE), with controlled surface roughness achieved via varying grit sizes. The findings advance the mechanical performance of single-lap joints in Type-IV tanks, offering reliable bonding methods for industrial applications. These results serve as a valuable resource for researchers, engineers, and manufacturers in materials engineering.

2. MATERIALS AND METHODS (MATERYAL VE METOD)

In this study, which focuses on the bonding of cured CFRP and HDPE plates, the CFRP plates were manufactured using epoxy-matrix prepreg materials with a density of 500 gsm. Prior to production, the prepreg materials were stored in a deep freezer and were brought to room temperature for 2 hours after removal. Subsequently, they were laminated in layers and cured under vacuum in a PLC-controlled heating oven at a curing rate of 5°C/min until reaching a target temperature of 120°C, where they were maintained for 2 hours. This process resulted in 5 mm thick CFRP plates. All test specimens used in the bonding experiments were cut from the same plate. Following this, bonding and adhesion performance were

evaluated using two commercially available, proven structural adhesives (DP460 and DP190) and compared with a commonly used commercial epoxy set, specifically the Hexion brand MGS Lamination Epoxy System L285/H287.

Composite plates were cut into shapes and dimensions specified by the ASTM D568 standard using a CNC router, making them suitable for bonding. To enhance the adhesion strength (optimize surface roughness) of the surfaces where HDPE would be bonded with the carbon plate, a sanding process was applied. Sandpapers with grit sizes of 120, 180, and 240, which have been reported to yield the best results in improving adhesion strength, were used [47–49]. Finally, the surfaces were subjected to sandblasting and cleaned with thinner.

Table 1. Properties of DP190 and DP460 Adhesives (DP190 ve DP460 Yapıştırıcıların Özellikleri)

Adhesive Type	DP190	DP460
Cure Time	7 day	7 day
Shear Strength	55°C'de 24 MPa	55°C'de 31 MPa
Strain	%30	-
Tensile Strength	24.1317 MPa	-
Viscosity	150 Pa/sec	275 Pa/sec
Max. Operating Temperature	+24°C	+23°C

Each sample, measuring 25.4 x 101.6 mm, was bonded using pure epoxy and two different adhesives (DP190 and DP460) from the 3M Scotch-Weld brand. The schematic representation of the bonded specimens is shown in Figure 1.

In order to ensure balanced load transfer and minimize any potential misalignment or thickness-induced stress concentrations during tensile testing, the tab regions were prepared by bonding CFRP and HDPE plates of equal surface area on both ends of the specimens. This configuration was deliberately chosen prior to testing to eliminate the effects of possible thickness mismatches between the two materials. By using identical bonding dimensions and surface preparations, a symmetrical geometry was achieved, allowing both tab ends to contribute equally to the load transfer during mechanical testing. This hybrid tab design was also intended to prevent premature failure or damage at the tab interfaces, which is a critical factor in obtaining reliable test results.

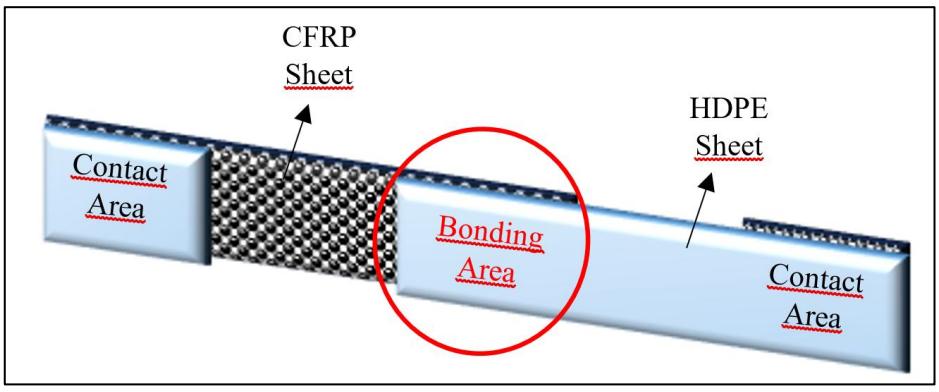

Figure 1. Single-Lap Joint Tensile Test Specimen. (Tek bindirmeli çekme testi numunesi)

The manufacturer states that DP190 and DP460 adhesives, whose technical specifications are given in Table 1., provide high strength by forming robust bonds in metal, plastic, and composite joints. These adhesives (particularly when surface preparation is applied) have also significantly improved bonding strength in HDPE joints [50].

To ensure consistent axial alignment during lap shear testing, particular attention was paid to the bonding stage of specimen preparation. All composite and HDPE plates were assembled on a flat reference surface, and a standardized alignment template was used to control the overlap length and maintain consistent positioning of the adherends. This manual alignment procedure was applied

uniformly across all specimens to minimize potential eccentricities and misalignments during subsequent mechanical testing. Although no specialized mechanical fixture was employed during the tensile tests, this careful assembly method provided a reliable and repeatable alignment across the test set. The adhesive bonding length in the joints was selected as 25.4 mm to prevent deformation from occurring in the lower layers. A universal tensile testing machine manufactured by UTEST was used to analyse the single-lap joints. The test specimens, as shown in Figure 2, were placed in the grips of the universal testing machine and subjected to tensile testing at a speed of 1.3 mm/min until failure. Tensile tests play a crucial role in evaluating the strength of single-lap joints.

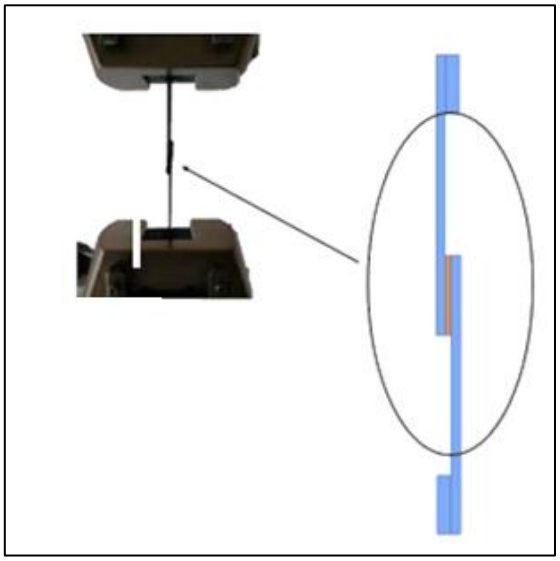

Figure 2. Schematic representation of the specimen during tensile testing (Çekme testi sırasında numunenin şematik gösterimi)

To prevent eccentric loading (reduce bending loads), the ends of the specimens were supported with additional parts to create gripping areas.

3. FINDINGS AND DISCUSSION (BULGULAR VE TARTIŞMA)

3.1. Mechanical Analysis Results (Mekanik Analiz Sonuçları)

This study evaluated how the bonding properties of composite structures vary depending on adhesive type and surface roughness. Five specimens were fabricated and tested for each sandpaper grit size. The obtained results were analyzed through graphical representation. A summary table of tensile test results is provided in Table 2.

Table 2. Tensile test data- summary table (Çekme testi verileri – özet tablo)

Sandpaper Grit Size	Shear Stress (MPa)		
	Epoxy	DP 190	DP 460
E-Un	2.1	2	1.2
120	3	25	1.9
180	2.5	13	2.1
240	12	12.8	1

For DP 190 adhesive, the standard deviation values calculated for E-Un, 120, 180, and 240 test coupons were 0.08, 0.01, 0.1, and 0.1 MPa, respectively. According to Figure 3., the use of 120-grit sandpaper on specimens bonded with DP190 provided the highest strength [51]. For specimens

bonded with DP190 without sanding, the shear stress was measured at approximately 2 MPa, with an elongation of 0.5%. This indicates that unsmoothed surfaces significantly limit bonding performance. In the DP190-120 specimen (sanded with 120-grit), the shear stress increased from 2 MPa to 25 MPa, while elongation rose from 0.5% to 2.3%, showing a significant improvement. This demonstrates that surface roughening with 120-grit sandpaper enhances both mechanical interlocking and bonding performance. Similarly, Kinloch's study emphasized that controlled surface roughness after sanding increases both strength and elongation capacity [52].

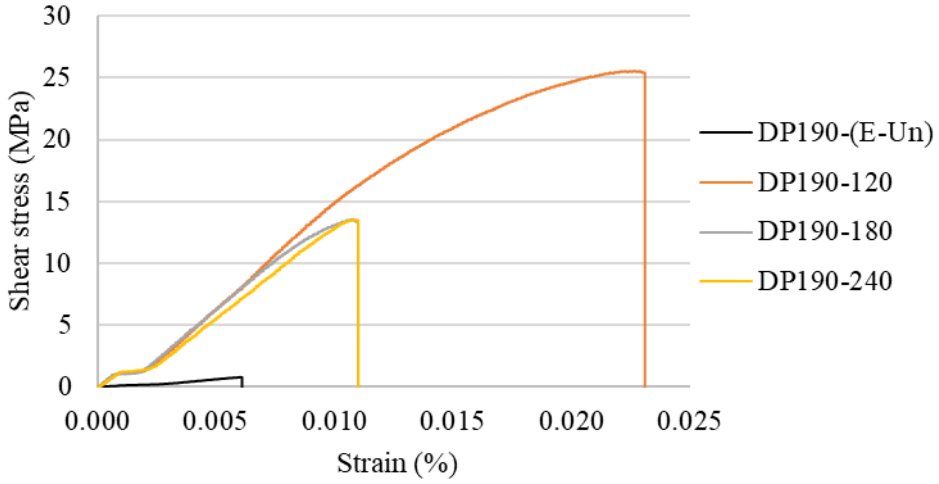

Figure 3. Shear stress-strain curve of the specimen bonded with DP190 and processed with different sandpaper grit sizes (Farklı zımpara numaralarıyla işlenmiş ve DP190 ile yapıştırılmış numunenin kesme gerilmesi-gerinim eğrisi.)

For DP 460 adhesive, the standard deviation values for E-Un, 120, 180, and 240 test specimens were determined as 0.02, 0.1, 0.1, and 0.1 MPa, respectively. Figure 4 shows that for the DP190-180 specimen (sanded with 180-grit), the shear stress increased to ~13 MPa compared to the unsanded specimen (E-Un), with elongation reaching 1.2%. However, the performance of 180-grit sandpaper was lower compared to 120-grit. The DP190-240 specimen (sanded with 240-grit) exhibited a similar curve to DP190-180.

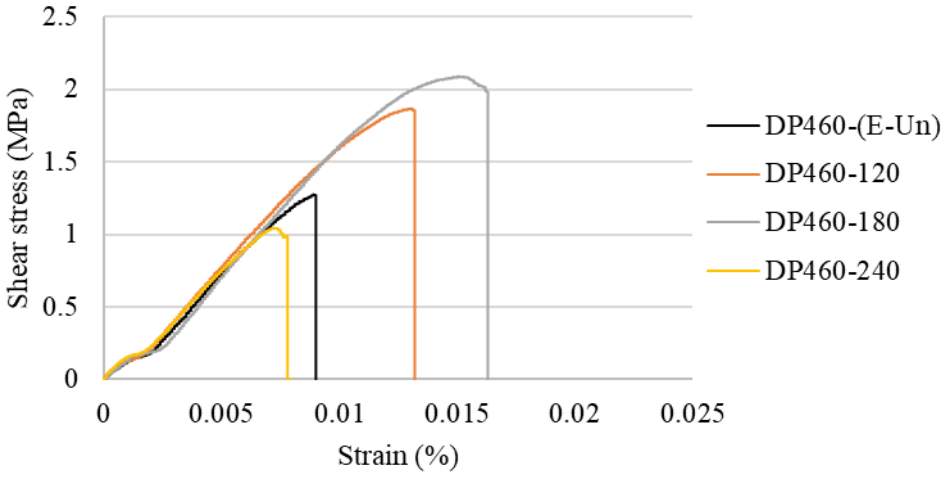

Figure 4. Shear Stress-Strain Curves of Specimens Bonded with DP460 (DP460 ile yapıştırılmış numunelere ait kesme gerilmesi-gerinim eğrileri)

The shear stress-strain curves of specimens bonded using DP460 adhesive are shown in Figure 4. According to the results, the DP460-(E-Un) specimen exhibited a shear stress of 1.2 MPa and an elongation of 0.8%. Compared to other specimens, the unsanded surface significantly limited bonding

performance, reducing mechanical interlocking and adhesion strength. When comparing the DP460-120 specimen to the unsanded specimen, the shear stress increased by approximately 58%, reaching 1.9 MPa, and the elongation rose by about 75% to 1.4%. The use of 120-grit sandpaper notably improved bonding strength by enhancing mechanical interlocking. The DP460-180 specimen demonstrated the best performance among the samples. Its shear stress increased by approximately 75% to 2.1 MPa, and elongation reached 1.6%. This improvement can be attributed to achieving optimal surface roughness, as expressed in ASTM D4541-17, allowing the adhesive to achieve maximum adhesion. In contrast, the DP460-240 specimen showed a decrease in shear stress of approximately 16%, dropping to 1.0 MPa, and a reduction in elongation of about 10%, reaching 0.7%. Accordingly, for DP 460 adhesive applications, it has been observed that surface preparation with excessively fine-grit abrasives fails to achieve adequate mechanical interlocking.

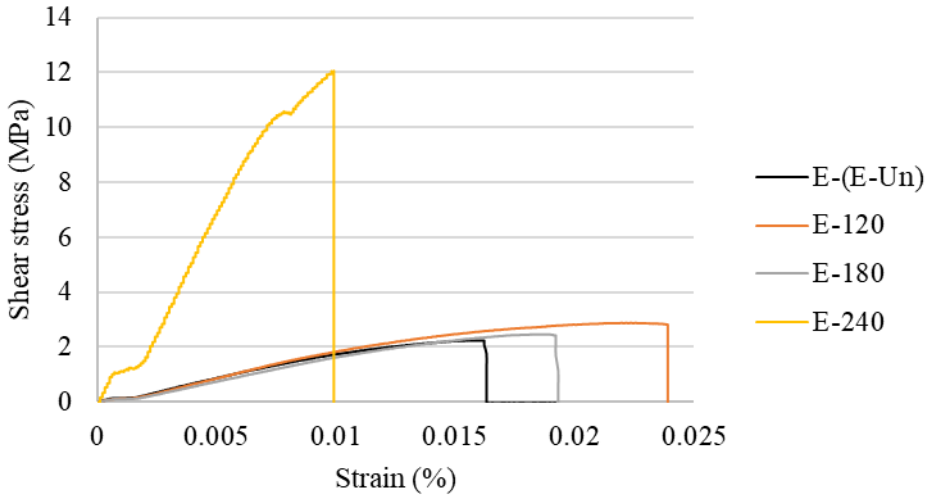

Figure 5. Shear Stress-Strain Curves of Specimens Bonded with Epoxy (Epoksi ile yapıştırılmış numunelere ait kesme gerilmesi-gerinim eğrileri).

For the epoxy adhesive, the standard deviation values for E-Un, 120, 180, and 240 test specimens were calculated as 0.03, 0.04, 0.08, and 0.04 MPa, respectively. The shear stress-strain graphs for specimens bonded with epoxy are presented in Figure 5. The specimen bonded without sanding exhibited a shear strength of ~2.1 MPa and an elongation of 1.6%, resulting in the lowest shear strength and limited elongation capacity. This indicates that epoxy bonding is significantly affected by surface preparation. For the specimen sanded with 120-grit sandpaper, the shear stress was ~3 MPa, and the elongation reached 2.4%. The controlled surface roughness provided a stronger adhesion capacity. The surface prepared with 180-grit sandpaper exhibited a shear stress of ~2.5 MPa and an elongation capacity of 1.9%, offering a balanced performance. The E-240 specimen, with finer surface roughness, showed both higher maximum stress (12 MPa) and shorter elongation (1%). This indicates that a finer surface roughness for the epoxy adhesive results in a structure with higher strength but lower elongation capacity. [53, 54].

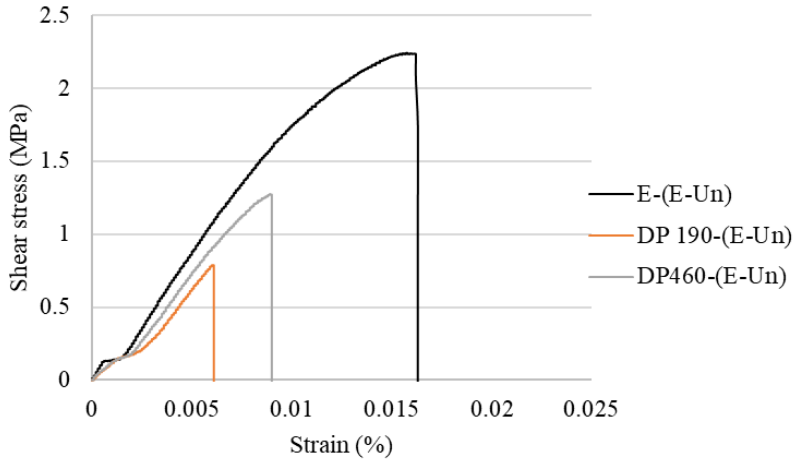

Figure 6. The Effect of Adhesive Type on Shear Stress (Yapıştırıcı türünün kesme gerilmesi üzerindeki etkisi).

As shown in Figure 6. the E-(E-Un) specimen (bonded with epoxy) exhibited the highest maximum shear stress (~2.3 MPa) and the greatest elongation capacity (1.6%). Consequently, the epoxy adhesive demonstrates superior shear stress and elongation characteristics compared to DP190 and DP460 adhesives, indicating its enhanced mechanical properties and high deformation capacity [55]. The DP190 adhesive exhibits the lowest maximum shear stress (~0.8 MPa) and elongation capacity (~0.5%), suggesting its suitability for low-strength applications. The DP460 adhesive shows intermediate performance between E-(E-Un) and DP190, with ~1.4 MPa shear stress and 0.8% elongation – representing a 75% higher shear strength and 60% greater elongation capacity than DP190. These results demonstrate DP460's applicability in medium-to-high strength applications. The findings align with material properties reported in literature for DP190 and DP460 [54].

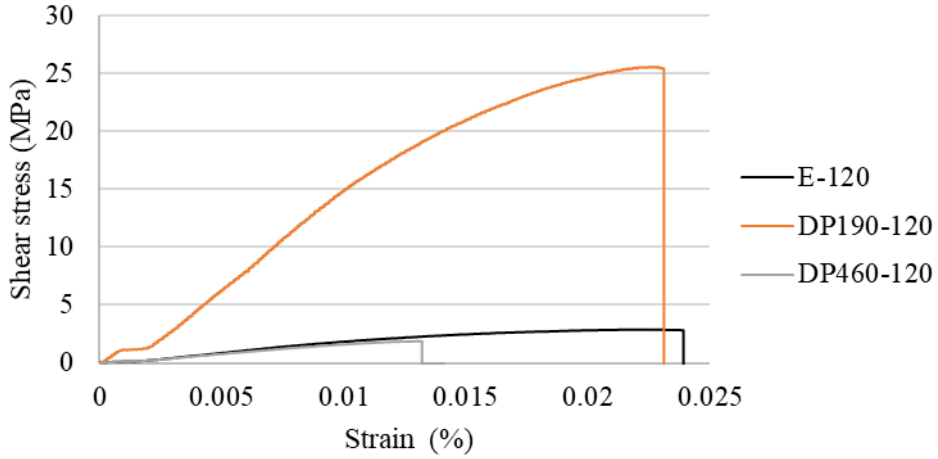

Figure 7. The Effect of Adhesive Type on Shear Stress in Specimens Processed with 120-Grit Sandpaper
(120 numara zımpara ile işlenmiş numunelerde yapıştırıcı türünün kesme gerilmesine etkisi) .

Figure 7. presents E-120 demonstrated a shear stress of ~3 MPa with ~2.4% elongation. While exhibiting lower shear stress compared to DP190-120, it outperformed DP460-120.

DP190 achieved the highest maximum shear stress (~25 MPa) and greatest elongation capacity (~2.2%), indicating its superior bonding performance and effective energy absorption capability on 120-grit abraded surfaces. It showed significantly better performance than both E-120 and DP460-120 in both shear stress and elongation. DP460 displayed the lowest maximum shear stress (~2 MPa) and elongation capacity (~1.3%), revealing its relatively weak performance on 120-grit surfaces. Compared to E-120, DP460 showed 33% lower shear stress and 45% reduced elongation capacity. DP190 generally exhibits higher elasticity and energy absorption capacity. DP460 provides greater rigidity but shows less sensitivity to surface

roughness variations [56] DP190-120 demonstrated optimal performance in both shear stress and elongation metrics, confirming its excellent surface compatibility when used with 120-grit abrasion treatment.

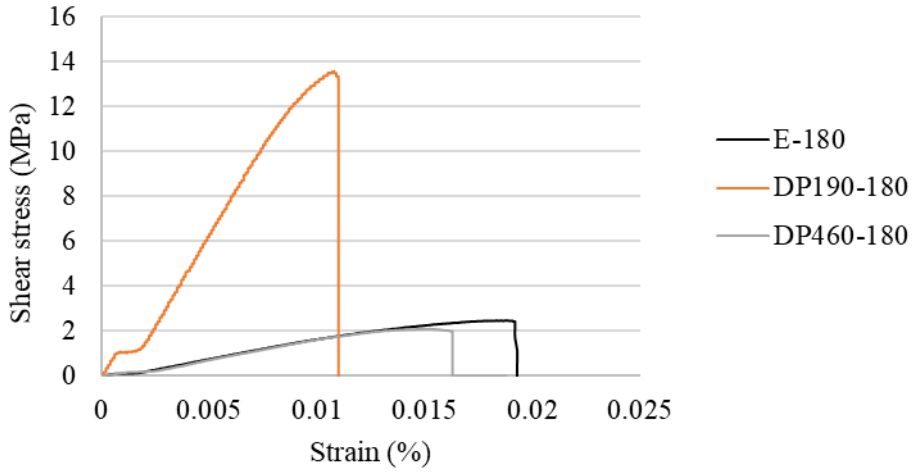

Figure 8. The Effect of Adhesive Type on Shear Stress in Specimens Processed with 180-Grit Sandpaper
(180 numara zımpara ile işlenmiş numunelerde yapıştırıcı türünün kesme gerilmesine etkisi).

Figure 8. presents the shear stress-elongation curves of test specimens prepared with 180-grit abrasion, showing adhesive performance effects. The epoxy-bonded specimen (E-180) initially exhibited gradual shear stress increase, reaching maximum values of approximately 2.5 MPa shear stress and 2% elongation. E-180 demonstrated approximately 100% greater deformation capacity compared to DP190. DP190 adhesive achieved the highest shear stress performance (~14 MPa), showing 460% greater strength than the epoxy adhesive at maximum shear stress. However, DP190 displayed limited deformation capacity, reaching maximum shear stress at only ~1.2% elongation. For DP460 adhesive, maximum values measured ~2 MPa shear stress and ~1.8% elongation - representing 20% lower shear stress and 10% reduced deformation capacity compared to E-180.

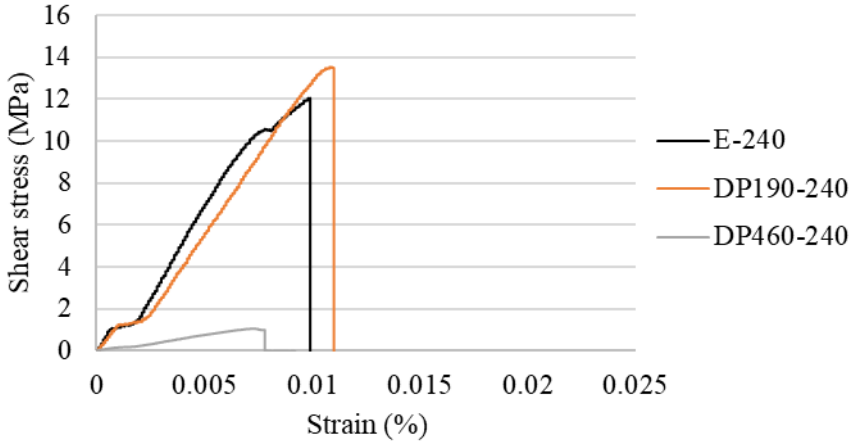

Figure 9. The Effect of Adhesive Type on Shear Stress in Specimens Processed with 240-Grit Sandpaper
(240 numara zımpara ile işlenmiş numunelerde yapıştırıcı türünün kesme gerilmesine etkisi) .

According to Figure 9., E-240 (epoxy adhesive) reached maximum shear stress of approximately 12 MPa with 1.1% elongation. Compared to E-180 (using 180-grit), E-240 showed a 380% increase in shear stress but a 45% reduction in elongation capacity. For DP190-240 adhesive, maximum shear stress measured 14 MPa with 1.2% elongation - showing no change in deformation capacity or

strength improvement versus 180-grit DP190. The DP460 adhesive demonstrated maximum shear stress of ~1 MPa and ~0.8% elongation capacity.

3.2. Fracture Surface Analysis (Kopma Yüzeyi Analizi)

For comprehensive analysis of tensile test results, examination of failure modes at bonding interfaces is essential. In adhesive-bonded joints, failures are characterized as either adhesive or cohesive failure. Adhesive failure refers to separation at the adhesive/substrate interface, while cohesive failure indicates internal fracture within the adhesive material itself. Figures 10., 11., and 12. present visual documentation of fracture surfaces from tested specimens.

a) b) c) d)

Figure 10. Fracture surfaces of epoxy-bonded specimens (Epoksi ile yapıştırılmış numunelerin kopma yüzeyleri) .
a) E-Un, b) E-120, c) E-180, d) E-240

Figure 10. clearly demonstrates that the non-abraded specimen failed via adhesive failure. For E-120 and E-180 specimens, mixed adhesive/cohesive failure modes were observed. While E-240 specimens showed increased cohesive failure characteristics, the dominant failure mode remained adhesive. All epoxy-bonded specimens ultimately failed at the HDPE surface interface, indicating superior epoxy adhesion to the CFRP substrate.

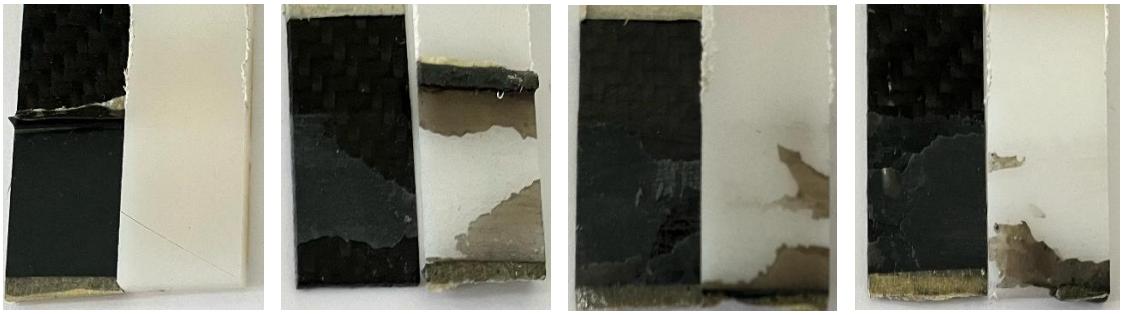

a) b) c) d)

Figure 11. Fracture surfaces of specimens bonded with DP-190 adhesive (DP-190 yapıştırıcısı ile birleştirilmiş numunelerin kırılma yüzeyleri) :

a) E-Un, b) E-120, c) E-180, d) E-240

As observed in Figure 11., the non-abraded specimen exhibited adhesive failure similar to the epoxy-bonded case, confirming DP 190's effective adhesion to CFRP surfaces. Visual analysis revealed optimal bonding performance in DP 190-180 specimens, while all abraded specimens demonstrated mixed adhesive/cohesive failure modes. Cohesive failure patterns were observed simultaneously on both CFRP and HDPE surfaces, indicating that surface abrasion enhances DP 190 adhesive's bonding performance with HDPE substrates.

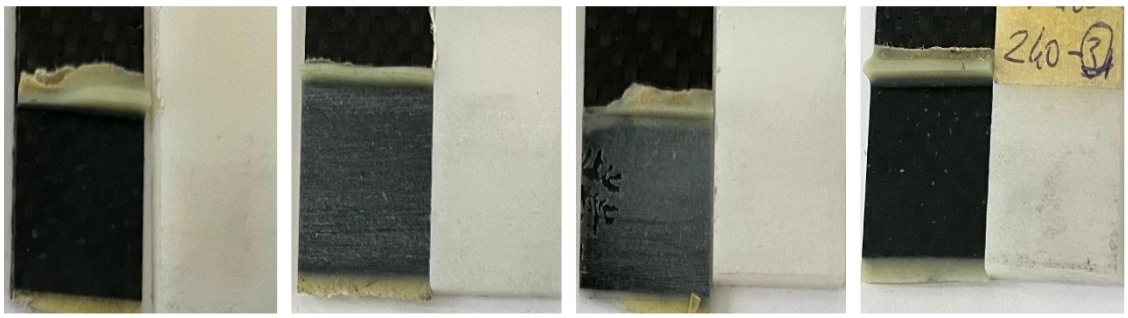

a) b) c) d)

Figure 12. Fracture surfaces of specimens bonded with DP-460 adhesive (DP-460 yapıştırıcısı ile birleştirilmiş numunelerin kırılma yüzeyleri):

a) E-Un, b) E-120, c) E-180, d) E-240

Figure 12. demonstrates that in DP 460 adhesive joints, both non-abraded specimens and DP 460-240 specimens failed via adhesive failure, indicating DP 460's effective bonding with CFRP. However, DP 460-120 and DP 460-180 specimens exhibited mixed adhesive/cohesive failure modes, with cohesive failure becoming more pronounced in DP 460-180 specimens. Critically, all specimens ultimately failed at the HDPE interface, revealing DP 460's poor adhesion compatibility with HDPE substrates.

3.2. SEM Analysis Results (SEM Analiz Sonuçları)

In structures formed by bonding thermoset-based composite materials with HDPE, the significant causes of failure identified via SEM analysis during tensile testing are the blister effect and fiber-matrix separation [57]. Fiber-matrix separation is one of the primary mechanisms of fracture [58]. In SEM images related to this effect, the exposure of fibers and their detachment from the matrix material are notable. The bubbles observed in SEM (scanning electron microscope) images, known as 'blisters,' typically result from voids or gas accumulations within the material's internal structure [53]. This effect significantly reduces the material's strength. Blister formations generally arise from weaknesses at the adhesive interface, gas bubbles present in the adhesive, or incompatibility between materials [59].

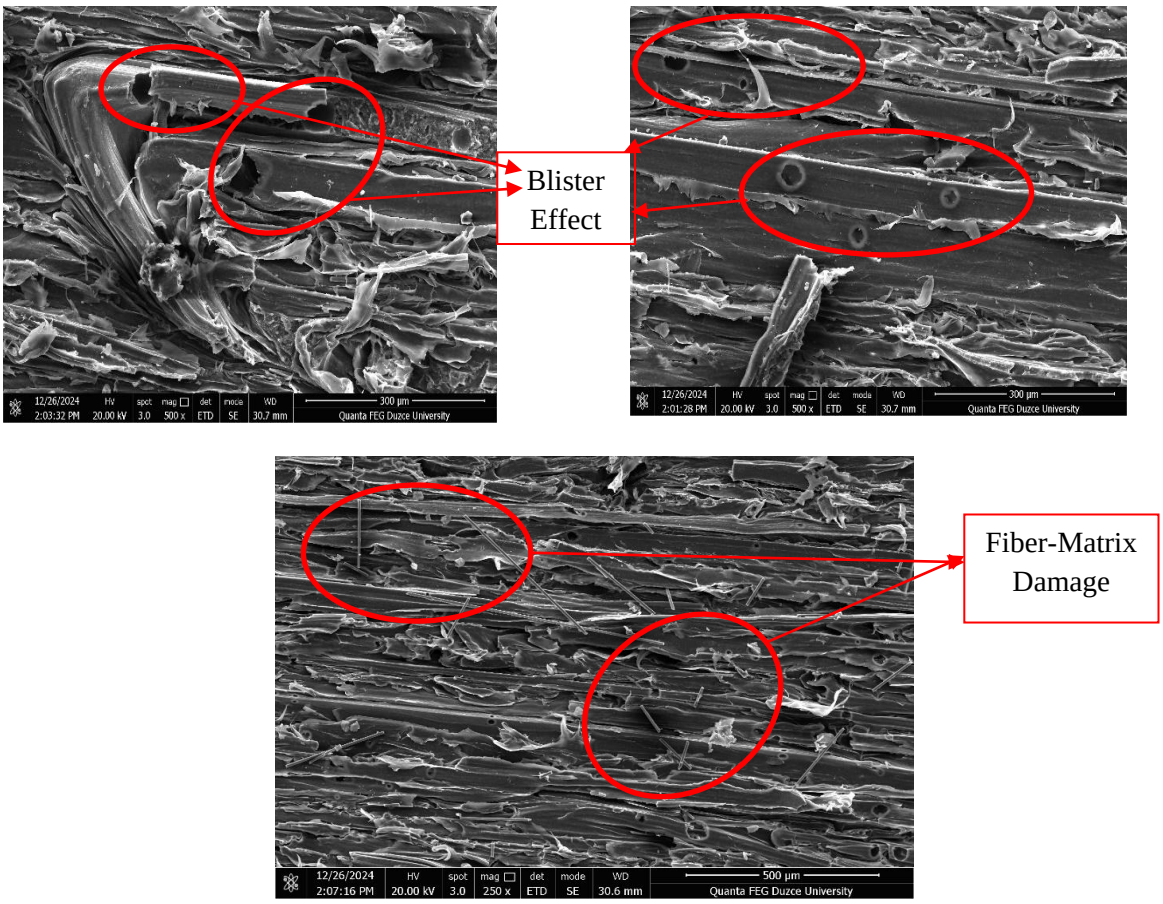

Figure 13. SEM Images of the specimen bonded with DP190 adhesive without surface preparation (Yüzey hazırlığı yapılmamış, DP190 yapıştırıcısı ile birleştirilmiş numuneye ait SEM görüntüleri).

When evaluating the data obtained from the mechanical tests, the highest shear stress results were achieved in the samples using DP190 adhesive with surface preparation. In the SEM images provided in Figure 13., blister bubbles and fiber-matrix damage in the bonded area, which contribute to this effect, are clearly visible.

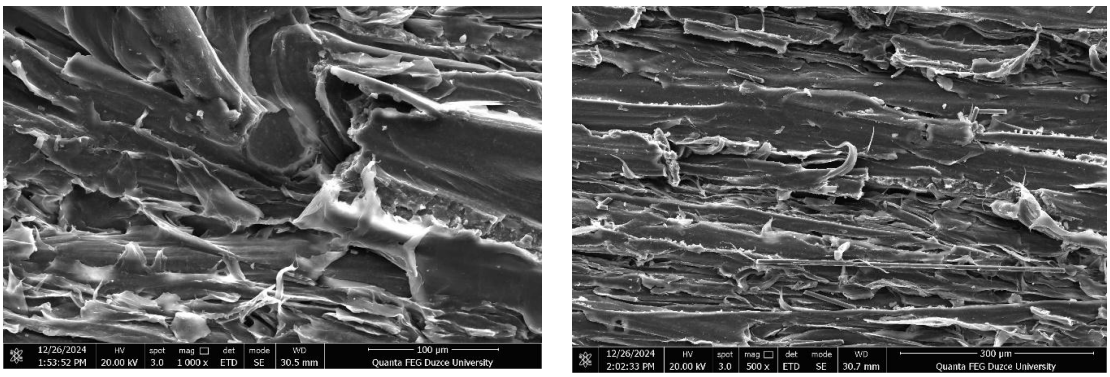

a) b)

Figure 14. 100x and 300x zoomed SEM Images of the sample bonded with DP190 adhesive: a) Sample treated with 180-grit sandpaper, b) Sample treated with 240-grit sandpaper (DP190 yapıştırıcısı ile birleştirilmiş numuneye ait 100x ve 300x büyütülmüş SEM görüntüleri: a) 180 numara zımpara ile işlenmiş numune, b) 240 numara zımpara ile işlenmiş numune).

Although the shear stress shows a decrease with 180 and 240-grit sandpaper treatment compared to 120-grit, it still remains at a higher level than untreated surfaces. No blister effect was observed in the SEM images presented in Figure 14.

4.CONCLUSION (SONUÇLAR)

According to the results obtained from the study, it is observed that surface preparation directly affects the bonding performance of composite materials and that optimal sanding thicknesses may vary depending on the type of adhesive. To ensure optimal bonding properties, the selection of adhesive type and surface preparation should be carefully made based on application requirements. The detailed findings are as follows.

• For DP190 and DP460 adhesives, optimal performance was achieved at 120-grit and 180-grit sanding, respectively. For DP460, excessive surface roughness or unsanded surfaces negatively affect bond strength. In epoxy-bonded joints, 120-grit sanding provided the most balanced performance, while 240-grit sanding resulted in notably high shear stress.

• Across all adhesive types, the lowest performance was observed in unsanded specimens due to insufficient surface preparation.

• Epoxy can be used for HDPE-CFRP bonding, but it does not provide as high strength as DP 190.

• DP 190 demonstrated strong adhesion with CFRP and, with proper mechanical surface preparation, also bonded well with HDPE. Additionally, due to its flexible nature, it is expected to better accommodate the thermal behavior of HDPE.

• DP460 was not found suitable for HDPE-CFRP bonding. It should instead be preferred for stiffer structural applications (e.g., metal-CFRP) under light loads.

In the present study, the elongation values presented in the stress–strain graphs are expressed in percentage (%), and the initial version of the manuscript contained a unit error, which has been corrected. It is important to note that the measured elongation reflects the global deformation behavior of the bonded joints, including the adhesive and substrates. While no extensometer was used along the bondline, the displacement data were obtained from the universal testing machine via crosshead movement. Therefore, the elongation values represent an integrated response rather than the local strain at the adhesive interface. A separate tensile test for the unbonded composite substrates was not conducted within the scope of this study; however, the difference in elongation between adhesive types indirectly reflects their influence on joint flexibility and strain accommodation. In future studies, inclusion of reference data for the neat composites and localized strain measurement tools such as digital image correlation (DIC) or bondline extensometers would provide more detailed insights into adhesive behavior under shear loading.

ACKNOWLEDGMENTS (TEŞEKKÜR)

This paper was supported by the Duzce University Scientific Research Projects (DUBAP) under grant 2024.06.05.1466 project number and Kompozit Malzemelerde Yapıştırma Yöntemlerinin İncelenmesi Project name.

AUTHORS' CONTRIBUTIONS (YAZARLARIN KATKILARI)

***Emin Öztürk*:** He conducted the experiments, analyzed the results and performed the writing process.
Deneyleri yapmış, sonuçlarını analiz etmiş ve maklenin yazım işlemini gerçekleştirmiştir.
Mert Kılınçel: He analyzed the results.
Sonuçları analiz etti.
Gülden Kabakçı: She performed the writing process.
Yazım sürecini gerçekleştirdi.
Ahmet Kömürcü: He conducted the experiments, analyzed the results and performed the writing process.
Deneyleri yapmış, sonuçlarını analiz etmiş ve maklenin yazım işlemini gerçekleştirmiştir.

CONFLICT OF INTEREST (ÇIKAR ÇATIŞMASI)

There is no conflict of interest in this study.
Bu çalışmada herhangi bir çıkar çatışması yoktur.

REFERENCES (KAYNAKLAR)

[1]Fava RA. Polymers (1980). Part C, Physical Properties Methods of Experimental Physics ; V. 16. 1,554

[2] Nielsen LE. Models for the Permeability of Filled Polymer Systems. Journal of Macromolecular Science: Part A - Chemistry. 1967; 1(5):929–42.

[3] Cussler EL, Hughes SE, Ward WJ, Aris R. Barrier membranes. J Memb Sci. 1988; 38(2):161–74.

[4] Kim HM, Lee JK, Lee HS. Transparent and high gas barrier films based on poly(vinyl alcohol)/graphene oxide composites. Thin Solid Films. 2011; 519(22):7766–71.

[5] Sun L, Boo WJ, Clearfield A, Sue HJ, Pham HQ. Barrier properties of model epoxy nanocomposites. J Memb Sci. 2008; 318(1–2):129–36.

[6] Drozdov AD, Christiansen J de C. Micromechanical modeling of barrier properties of polymer nanocomposites. Compos Sci Technol. 2020; 189.

[7] Huang HD, Ren PG, Xu JZ, Xu L, Zhong GJ, Hsiao BS, et al. Improved barrier properties of poly(lactic acid) with randomly dispersed graphene oxide nanosheets. J Memb Sci. 2014; 464:110–8.

[8] Minelli M, Baschetti MG, Doghieri F. Analysis of modeling results for barrier properties in ordered nanocomposite systems. J Memb Sci. 2009; 327(1–2):208–15.

[9] Huang HD, Ren PG, Chen J, Zhang WQ, Ji X, Li ZM. High barrier graphene oxide nanosheet/poly(vinyl alcohol) nanocomposite films. J Memb Sci. 2012; 409–410:156–63.

[10] Govindaraj P, Sokolova A, Salim N, Juodkazis S, Fuss FK, Fox B, et al. Distribution states of graphene in polymer nanocomposites: A review. 2021: Vol. 226, Composites Part B: Engineering.

[11] Carrera MC, Erdmann E, Destéfanis HA. Barrier properties and structural study of nanocomposite of HDPE/montmorillonite modified with polyvinylalcohol. Journal of Chemistry.Vol. 2013; 1-7.

[12] Rueda F, Marquez A, Otegui JL, Frontini PM. Buckling collapse of HDPE liners: Experimental set-up and FEM simulations. Thin-Walled Structures. 2016; 109:103–12.

[13] Li X, Tabil LG, Oguocha IN, Panigrahi S. Thermal diffusivity, thermal conductivity, and specific heat of flax fiber-HDPE biocomposites at processing temperatures. Compos Sci Technol. 2008; 68(7–8):1753–8.

[14] Luo S, Fu J, Zhou Y, Yi C. The production of hydrogen-rich gas by catalytic pyrolysis of biomass using waste heat from blast-furnace slag. Renew Energy. 2017;101:1030–6.

[15] Warner M, Jeng T, Ayar S, Sekhar S, Marin D, Engler A, et al. Reduced graphene oxide catalytically enhances the rate of cyanate ester curing under variable frequency microwave heating. J Appl Polym Sci. 2023;140(21).

[16] Warner M, Jeng T, Ayar S, Sekhar S, Marin D, Engler A, et al. Reduced graphene oxide catalytically enhances the rate of cyanate ester curing under variable frequency microwave heating. J Appl Polym Sci. 2023;140(21).

[17] Ma Q, Rejab MRM, Azeem M, Hassan SA, Yang B, Kumar AP. Opportunities and challenges on composite pressure vessels (CPVs) from advanced filament winding machinery: A short communication. Int J Hydrogen Energy. 2024; 57:1364–72.

[18] Hu Z, Chen M, Pan B. Simulation and burst validation of 70 MPa type IV hydrogen storage vessel with dome reinforcement. Int J Hydrogen Energy. 2021;46(46):23779–94.

[19] Air A, Oromiehie E, Prusty BG. Design and manufacture of a Type V composite pressure vessel using automated fibre placement. Compos B Eng. 2023;266.

[20] Wang X, Tian M, Chen X, Xie P, Yang J, Chen J, et al. Advances on materials design and manufacture technology of plastic liner of type IV hydrogen storage vessel. Vol. 47, International Journal of Hydrogen Energy. Elsevier Ltd; 2022. p. 8382–408.

[21] Sharma P, Burolia AK, Adak NC, Daiya J, Sardar HH, Neogi S. Effect of tension on liner buckling and performance of a type-4 cylinder for storage of compressed gases with experimental validation. Thin-Walled Structures. 2023;189.

[22] Fang Q, Ji D. Molecular simulation of hydrogen permeation behavior in liner polymer materials of Type IV hydrogen storage vessels. Mater Today Commun. 2023;35.

[23] Condé-Wolter J, Ruf MG, Liebsch A, Lebelt T, Koch I, Drechsler K, et al. Hydrogen permeability of thermoplastic composites and liner systems for future mobility applications. Compos Part A Appl Sci Manuf. 2023;167.

[24] Condé-Wolter J, Ruf MG, Liebsch A, Lebelt T, Koch I, Drechsler K, et al. Hydrogen permeability of thermoplastic composites and liner systems for future mobility applications. Compos Part A Appl Sci Manuf. 2023;167.

[25] Hu Z, Chen M, Pan B. Simulation and burst validation of 70 MPa type IV hydrogen storage vessel with dome reinforcement. Int J Hydrogen Energy. 2021;46(46):23779–94.

[26] Sun Y, Lv H, Zhou W, Zhang C. Research on hydrogen permeability of polyamide 6 as the liner material for type IV hydrogen storage tank. Int J Hydrogen Energy. 2020;45(46):24980–90.

[27] Barthélémy H. Hydrogen storage - Industrial prospectives. Int J Hydrogen Energy. 2012;37(22):17364–72.

[28] Rueda F, Torres JP, Machado M, Frontini PM, Otegui JL. External pressure induced buckling

collapse of high density polyethylene (HDPE) liners: FEM modeling and predictions. Thin-Walled Structures. 2015;96:56–63.

[29] Rueda F, Otegui JL, Frontini P. Numerical tool to model collapse of polymeric liners in pipelines. Eng Fail Anal. 2012;20:25–34.

[30] Bo K, Feng H, Jiang Y, Deng G, Wang D, Zhang Y. Study of blister phenomena on polymer liner of type IV hydrogen storage cylinders. Int J Hydrogen Energy. 2024;54:922–36.

[31] Huang HD, Ren PG, Xu JZ, Xu L, Zhong GJ, Hsiao BS, et al. Improved barrier properties of poly(lactic acid) with randomly dispersed graphene oxide nanosheets. J Memb Sci. 2014;464:110–8.

[32] Bo K, Feng H, Jiang Y, Deng G, Wang D, Zhang Y. Study of blister phenomena on polymer liner of type IV hydrogen storage cylinders. Int J Hydrogen Energy. 2024;54:922–36.

[33] Blanc-Vannet P, Papin P, Weber M, Renault P, Pepin J, Lainé E, et al. Sample scale testing method to prevent collapse of plastic liners in composite pressure vessels. Int J Hydrogen Energy. 2019;8682–91.

[34] Mariscal G, Depcik C, Chao H, Wu G, Li X. Technical and economic feasibility of applying fuel cells as the power source of unmanned aerial vehicles. Energy Convers Manag. 2024;301.

[35] Liu M, Lin K, Zhou M, Wallwork A, Bissett MA, Young RJ, et al. Mechanism of gas barrier improvement of graphene/polypropylene nanocomposites for new-generation light-weight hydrogen storage. Compos Sci Technol [Internet]. 2024;110483.Availablefrom:https://linkinghub.elsevier.com/retrieve/pii/S0266353824000538

[36] Su Y, Lv H, Feng C, Zhang C. Hydrogen permeability of polyamide 6 as the liner material of Type IV hydrogen storage tanks: A molecular dynamics investigation. Int J Hydrogen Energy. 2024;50:1598–606.

[37] Sapre S, Pareek K, Vyas M. Investigation of structural stability of type IV compressed hydrogen storage tank during refueling of fuel cell vehicle. Energy Storage. 2020;2(4).

[38] Liu G, Zhang X, Yang Z, Wang L, Yang F, Wang R. Effects of interfaces and ordered microstructures on thermal properties of graphene flakes/polyethylene composites. Polym Compos. 2023;44(2):1371–80.

[39] Blanco-Aguilera R, Martinez-Agirre M, Berasategi J, Penalba M, Bou-Ali MM, Shevtsova V. Effect of liner thermal properties and liner pre-cooling on the thermal management of fast-filling of hydrogen tanks. Int J Hydrogen Energy. 2024;52:1159–72.

[40] Drozdov AD, Christiansen J de C. Micromechanical modeling of barrier properties of polymer nanocomposites. Compos Sci Technol. 2020;189.

[41] Balasooriya W, Clute C, Schrittesser B, Pinter G. A Review on Applicability, Limitations, and Improvements of Polymeric Materials in High-Pressure Hydrogen Gas Atmospheres. Vol. 62, Polymer Reviews. Taylor and Francis Ltd.; 2022. p. 175–209.

[42] K. Nemani et al., “Surface Modification: Surface Modification of Polymers: Methods and Applications (Adv. Mater. Interfaces 24/2018),” Adv. Mater. Interfaces, vol.5,2018, doi: 10.1002/admi.201870121.

[43] E. M. Liston, M. L., and M. R. and Wertheimer, “Plasma surface modification of polymers for improved adhesion: a critical review,” J. Adhes. Sci. Technol., vol. 7, no. 10, pp. 1091–1127, 1993, doi: 10.1163/156856193X00600.

[44] Pizzi, A., & Mittal, K.L. (Eds.). (2003). Handbook of Adhesive Technology, Revised and Expanded (2nd ed.). CRC Press. https://doi.org/10.1201/9780203912225

[45] E. M. Petrie, Epoxy Adhesive Formulations. in McGraw Hill professional. McGraw Hill LLC, 2005; [Online]. Available: https://books.google.com.tr/books?id=738MPfO5FEkC

[46] A. J. Kinloch, Adhesion and adhesives: science and technology. Springer Science & Business Media, 1987;

[47] Yudhanto, Arief & Alfano, Marco & Lubineau, Gilles. Surface preparation strategies in secondary bonded thermoset-based composite materials: A review. Composites Part A Applied Science and Manufacturing. 2021; 147. 106443. 10.1016/j.compositesa.2021.106443.

[48] Nasiry Khanlar L, Revilla-León M, Barmak AB, Ikeda M, Alsandi Q, Tagami J, Zandinejad A. Surface roughness and shear bond strength to composite resin of additively manufactured interim restorative material with different printing orientations. J Prosthet Dent. 2023 May;129(5):788-795. doi: 10.1016/j.prosdent.2021.08.010. Epub 2021 Oct 1. PMID: 34602276.

[49] Budhe, S., Ghumatkar, A., Birajdar, N. et al. Effect of surface roughness using different adherend materials on the adhesive bond strength.

Appl Adhes Sci 3, 20 2015; https://doi.org/10.1186/s40563-015-0050-4.

[50] S. Saha, D. Kocaefe, Y. Boluk, V. Mshvildadze, J. Legault, and A. Pichette, "Boreal forest conifer extracts: potential natural additives for acrylic polyurethane coatings for the protection of heat-treated jack pine," J. Coatings Technol. Res., vol. 10, no. 1, pp. 109–122, 2013, doi: 10.1007/s11998-012-9435-5.

[51] M., Rawat, P., Sai, L., Behera, R. P., Singh, K. K., & Zhu, D. (2021). Shear performance of MWCNTs modified single-lap joints of glass/epoxy laminates . Journal of Adhesion Science and Technology, 36(22), 2418–2437. https://doi.org/10.1080/01694243.2021.2011825.

[52] Kinloch, A.J. (1987) Adhesion and Adhesives: Science and Technology. Chapman and Hall, London. http://dx.doi.org/10.1007/978-94-015-7764-9

[53] Naito, K., Hirakata, H., & Fuj, T. (1997). Effect of surface treatment for steel adherends on static and fatigue crack growth of epoxy adhesives. Composite Interfaces, 5(4), 345–361. https://doi.org/10.1163/156855498X00126..

[54] Dadian, A., Rahnama, S., & Zolfaghari, A. (2020). Experimental study of the CTBN effect on mechanical properties and mode I and II fracture toughness of a new epoxy resin. Journal of Adhesion Science and Technology, 34(22), 2389–2404. https://doi.org/10.1080/01694243.2020.1763540

[55] Kabakçı, G., Kılınçel, M. & Tezel, G.B. Nanofiller Effects on the Isothermal Curing Kinetics of Epoxy Resin. Theor Found Chem Eng 2023; 57,1490–1502. https://doi.org/10.1134/S004057952306009X.

[56] R. Sahin, S. Akpinar. The effects of adherend thickness on the fatigue strength of adhesively bonded single-lap joints, International Journal of Adhesion and Adhesives, 107, 2021. https://doi.org/10.1016/j.ijadhadh.2021.102845.

[57] Hernandez, D. A., Soufen, C. A., & Orlandi, M. O. (2017). Carbon fiber reinforced polymer and epoxy adhesive tensile test failure analysis using scanning electron microscopy. Materials Research, 20(4), 951-961.

[58] L. Scott Chumbley, Larry D. Hanke, Scanning Electron Microscopy for Failure Analysis, Failure Analysis and Prevention, Vol 11, 2021 ed., ASM Handbook, Edited By Brett A. Miller, Roch J. Shipley, Ronald J. Parrington, Daniel P. Dennies, ASM International, 2021; p 240–250, https://doi.org/10.31399/asm.hb.v11.a0006769

[59] Kobayashi, M., Ishikawa, T. and Takahara, A. (2013). Adhesion and Tribological Characteristics of Ion-Containing Polymer Brushes Prepared by Controlled Radical Polymerization. In Polymer Adhesion, Friction, and Lubrication, H. Zeng (Ed.). https://doi.org/10.1002/9781118505175.ch2